ENERGY AND EXERGY ANALYSIS OF DOUBLE EFFECT (PARALLEL AND SERIES FLOW) ABSORPTION CHILLER SYSTEMS

Yang, Hu, PhD Candidate, Carnegie Mellon University, Pittsburgh, PA, USA;
Laura, Schaefer, Associate Professor, University of Pittsburgh, Pittsburgh, PA, USA;
Volker, Hartkopf, Professor, Carnegie Mellon University, Pittsburgh, PA, USA

Abstract: In this paper, three double effect absorption chiller system models are developed. One is for parallel flow and the two are for series flow. These flow directions refer to the solution flowing from the absorber to the regenerators. Given the same amount of cooling capacity and the same set of environmental conditions (room, condensing and regenerating temperatures), the temperature, enthalpy, entropy, mass flow rate, and lithium bromide mass fraction in each component of the three absorption systems are presented, together with the exergy destruction calculations. The results show, as expected, that the exergy destruction/losses in the system reduce the system COPs compared to those of reversible cycles. Examining the exergy destruction in detail, it can be seen that the losses in the generator, absorber, and heat exchangers are significantly larger than those in evaporator, condenser and expansion valves. The series flow configuration, with the solution flowing to the low temperature regenerator, has the highest COP and exergetic efficiency, but is also most vulnerable to crystallization formation. From the combined analyses, the double effect parallel flow absorption chiller is the best in terms of system performance and avoidance of crystallization.

Key Words: energy, exergy, double effect absorption chiller, parallel flow, series flow

1 INTRODUCTION

Absorption chiller systems have been studied and developed for decades. However, there has recently been an increased interest in absorption chiller technology due to energy and environmental issues. The absorption chiller uses thermal energy instead of electricity to provide cooling, which greatly reduces the peak power load from the grid in the summer, and, at the same time, the lithium bromide solution has no global warming potential or ozone depleting potential. Unfortunately, a traditional single stage absorption chiller with a COP around 0.7 cannot complete with an electrical driven chiller with an average COP around 4. Thus, double and multiple-stage absorption chillers are being developed to achieve higher COPs.

There are a large number of publications on absorption cycles, but only the research most germane to this study is cited below. Herold et al. (1996) summarized the technology of absorption chillers from fundamental knowledge, to field applications, to energy system modeling. Arun et al. (2001) analyzed a double-effect parallel flow absorption refrigeration cycle with water–lithium bromide as the working fluid based on the concept of an equilibrium temperature at the low pressure generator. Arora et al. (2009) developed a computational model for the parametric investigation of single-effect and series flow double-effect LiBr/ H_2O absorption refrigeration systems.

Building on this work, in this paper, three double-effect absorption chiller configurations are introduced. They are a double effect chiller with parallel flow, a series flow chiller with the

solution flowing to the low temperature regenerator (LTRG) first, and a series flow chiller with the solution flowing to the high temperature regenerator (HTRG) first. All three configurations are modeled using a software program known as Engineering Equation Solver (EES). EES (Klein et al. 2010) is frequently used for absorption chiller modeling due to its iterative capabilities and comprehensive internal/external libraries for LiBr/ H_2O and NH_3/H_2O.

For the parallel flow case, the lithium bromide dilute solution after the absorber flows into the HTRG and LTRG at the same time in parallel. The lithium bromide strong solutions from the two regenerators do not mix together, but directly spray into the absorber. This configuration is shown in Figure 1. Note that the SHX units are solution heat exchangers.

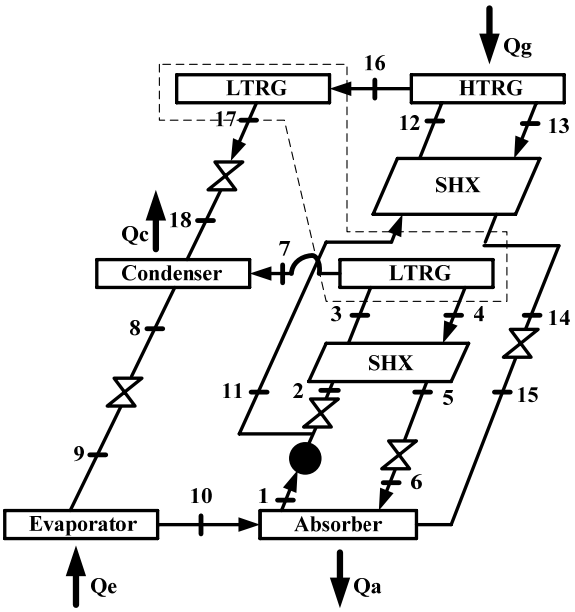

Figure 1: Double Effect Absorption Chiller with Parallel Flow

Figure 2 shows the first of the two series flow configurations. In this configuration, the lithium bromide dilute solution after the absorber first flows into the HTRG, and the strong lithium bromide solution passes through a solution expansion valve before it enters into the LTRG.

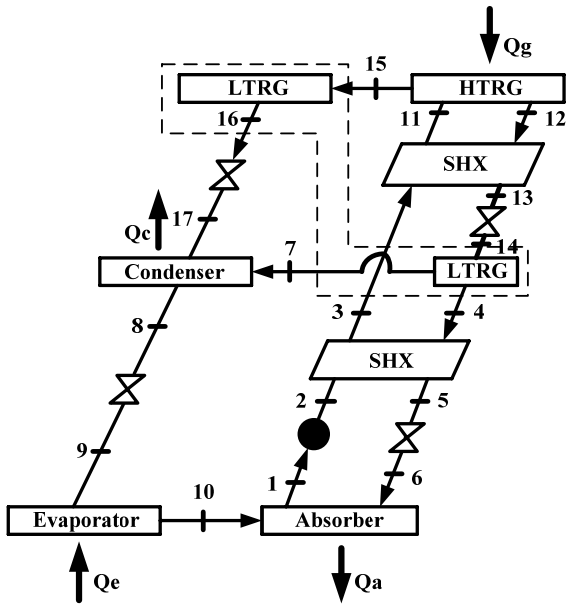

Figure 2: Double Effect Absorption Chiller with Series Flow (Solution to HTRG first)

The second series flow configuration to be evaluated is shown in Figure 3. In this configuration, the solution after absorber first enters into the LTRG and then into the HTRG.

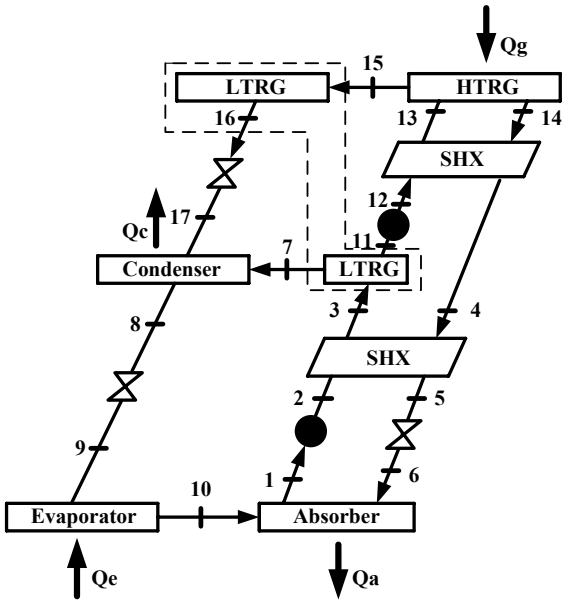

Figure 3: Double Effect Absorption Chiller with Series Flow (Solution to LTRG first)

In the following sections, the energy and exergy analyses for all three configurations is outlined and then performed. Next, the outcomes of these models are presented, and the pertinent results from all three configurations are discussed. Finally, conclusions are drawn from this discussion, and recommendations are presented.

2 MATHEMATICAL MODELLING

2.1 Theoretical Reversible Absorption Cycle

The Carnot cycle and reverse Carnot cycle can be combined and used to form an idealized absorption cycle. The ideal absorption cycle means it is a reversible cycle, and there is no entropy generation in the process, which is shown in Figure 4, below.

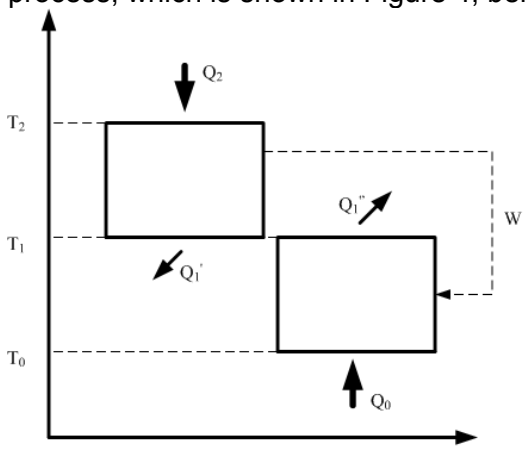

Figure 4: Theoretical Reversible Absorption Cycle

The Carnot cycle receives heat Q_2 at temperature T_2, and dumps the heat Q_1' to the environment while providing work W (= Q_2 - Q_1'). At the same time, the work W is used in the reverse Carnot cycle. The heat Q_0 is absorbed from the space to be cooled at temperature T_0,

and the heat Q_1'' (=Q_0+W) is released into the environment. The total absorption cycle efficiency is the multiplication of the Carnot and the reverse Carnot efficiencies, as shown in equation (1). This theoretical efficiency is the highest absorption chiller COP for the given set of environmental conditions (room, condensing, and regenerating temperatures). The theoretical COP, since there is no entropy generation, also signifies a 100% system exergetic efficiency.

$$COP_{rev} = \frac{T2-T1}{T2}\,\frac{T0}{T1-T0} \quad (1)$$

2.2 Energy Modeling

The principle of mass, species conservation, and the first law of thermodynamics are applied for each component of the various cycle configurations for energy modeling at steady state conditions. They can be written as follows:

$$\sum \dot{m}_i = \sum \dot{m}_o \quad (2)$$

$$\sum \dot{m}_i X_i = \sum \dot{m}_o X_o \quad (3)$$

$$\sum \dot{Q} - \sum \dot{W} = \sum \dot{m}_o h_o - \sum \dot{m}_i h_i \quad (4)$$

2.3 Exergy Modeling

By combing first law and second law of thermodynamics, the exergy balance for a control volume undergoing a steady state process can be written as follows (Lee et al. 1999), in terms of exergy destruction:

$$\dot{E}D_i = \sum(\dot{m}e)_{in} - \sum(\dot{m}e)_{out} + \sum \dot{Q}\left(1 - \frac{T_0}{T}\right) - \sum \dot{W} \quad (5)$$

The thermal exergy loss rate can be written as:

$$\dot{E}L_i = \dot{Q}_i\left(1 - \frac{T_0}{T_i}\right) \quad (6)$$

where $\dot{Q}_i$ is the heat rejected by the component (mainly the rejected heat from the absorber and condenser) and T_i is boundary temperature. Therefore, the total irreversibility at the component level can be expressed as:

$$\text{Irreversibility for each component} = \dot{E}D_i + \dot{E}L_i \quad (7)$$

3 ASSUMPTIONS

As described in detail below, certain assumptions can be made from documentation in the literature for the environmental conditions, absorber temperature, and LTRG temperature for all the three configurations. In addition to these assumptions, the cooling capacities are also fixed for all three configurations. The assumptions are as follows (note that all state points refer to those given in Figures 1-3):

i) The reference condition for exergy analysis is T_0 is 25 C and P_0 is 101.3 kPa;

ii) The pressure and heat losses through the system components are negligible;

iii) The solutions leaving the absorber and generators are saturated;

iv) The temperatures of the solutions leaving the absorber and LTRG are obtained from BCT16 (2005) for parallel flow (T [1] = 34 C and T [4] = 88 C) and for series flows: for the configuration where the solution flows to the HTRG first, T[1] = 34 C and T[4] = 88 C, and for the configuration where the solution flows to the LTRG first, T[1] = 34 C and T[11] = 88 C;

v) The refrigerant qualities leaving the condenser and evaporator are a saturated liquid and saturated vapor, respectively;

vi) The refrigerant leaving the high temperature generator is considered to be a superheated vapor at the high temperature generator temperature;

vii) The same cooling capacity (16 kW) is used for all three configurations;

viii) The same environmental temperatures are used for all three configurations, where the evaporator absorbs the heat from a room at 9 C, the condenser rejects the heat to the 40 C environment, and the high temperature regenerator absorbs heat from a 160 C heat source;

ix) There are 5 C temperature differences for absorbing and rejecting heat between the system points and the environment. So in parallel flow, T[10] =4 C, T[8]= 45 C, and T[13] = 155 C; in series flow to the HTRG first, T[10] = 4 C, T[8] = 45 C, and T[12] = 155 C; in series flow to the LTRG first, T[10] = 4 C, T[8] = 45 C and T[14] = 155 C;

x) The pumps are assumed to be isentropic pumps for ease of calculation;

xi) The lithium bromide solution expansion valves are near isentropic (a 0.0001 difference in value between two pressures) due to the limitations in the currently available literature.

For assumption x), the entropy calculation for lithium bromide in Engineering Equation Solver is based on Patek et al. (2006). There is no derived equation calculating the solution entropy based on pressure. In this paper, the solution expansion valves are considered as near isentropic with the same assumption as shown in Arora et al. (2009).

4 RESULTS

4.1 Theoretical Reversible Absorption Cycle and COP limitation

At the given reference conditions, by using equation 1 and a condensing temperature of 40 C and a regenerator temperature of 160 C, the limiting COP under this set of conditions is $COP_{rev} = 5.5$.

4.2 EES Model Validation by a Single Effect Absorption Chiller

As discussed in the assumptions, the expansion valves for the lithium bromide solution are considered to be near isentropic (a 0.0001 difference in value between the two pressures) due to the limitation of currently available research and the equations of state in the EES library. Before we analyze the energy and exergy absorption chiller model, the model itself has to be confirmed based on previous research. In Arora et al. (2009), one of the assumptions is that the solution expansion valve is near isentropic. Thus, a single effect absorption chiller model was created in EES based on parameters in Arora et al. (2009), and

the comparison results are shown Table 1. The difference is within 2.69% for the maximum and 0.003% for the minimum. Therefore, this single effect absorption chiller model is confirmed with Arora et al. (2009). Based on this single effect model, the three double effect absorption chiller models were then developed.

Table 1: EES Model Validation for a Single Effect Absorption Chiller

	Arora (2009)		EES Model Results		Difference	
Component	Energy (kW)	Exergy Destruction (kW)	Energy (kW)	Exergy Destruction (kW)	Energy %	Exergy Destruction %
Generator	3095.698	55.568	3093	54.07	-0.087	-2.69
Absorber	-2945.269	70.478	-2943	71.26	0.077	-0.31
Evaporator	2355.45	86.275	2355	84.97	-0.02	-1.51
Condenser	-2505.91	6.606	-2506	6.762	0.003	2.3
Solution heat exchanger	Adiabatic	25.081	Adiabatic	25.47	N/A	1.53
Solution valve	Adiabatic	0.02381	Adiabatic	0.02396	N/A	0.6
Refrigerant valve	Adiabatic	6.936	Adiabatic	6.925	N/A	0.159
Pump	0.03143	0.03143	0.03093	0.03093	0.002	0.002
COP	0.7609	N/A	0.7615	N/A	0.08	N/A

4.3 Double Effect Absorption Chiller with Parallel flow

The conservation equations outlined in Section 2.2 and the exergy balance equations described in Section 2.3 were applied to the double effect absorption chiller shown in Figure 1. The calculated results are shown in Table 2, and the resulting energy and exergy values and calculations are shown in Table 3. The reference points in both tables correspond to those given in Figure 1.

Table 2: State Points in Double Effect Absorption Chiller with Parallel Flow (Bold numbers are assumptions)

	P[kPa]	T[C]	X[%LiBr]	M[kg/sec]	H[kJ/kg]	S[kJ/kgK]
1	0.8136	**34**	55.35	0.08043	83.57	0.2044
2	9.59	34	55.35	0.04862	83.61	0.2045
3	9.59	58.89	55.35	0.04862	134.1	0.3629
4	9.59	**88**	58.64	0.0459	204.5	0.5071
5	9.59	61	58.64	0.0459	151	0.3534
6	0.8136	61	58.64	0.0459	151	0.3535
7	9.59	69.73		0.002724	2629	8.306
8	9.59	**45**		0.006898	188.3	0.6385
9	0.8136	4		0.006898	188.3	0.6798
10	0.8136	**4**		0.006898	2508	9.049
11	75.3	34	55.35	0.03181	83.61	0.2044
12	75.3	82.34	55.35	0.03181	182.8	0.5042
13	75.3	**155**	63.71	0.02763	355.7	0.7913
14	75.3	94.5	63.71	0.02763	241.5	0.5043
15	0.8136	94.5	63.71	0.02763	241.5	0.5044
16	75.3	**155**		0.004174	2788	7.77
17	75.3	91.89		0.004174	384.9	1.214
18	9.59	44.97		0.004174	384.9	1.256

Table 3: Energy/ Exergy Calculations for Double Effect Absorption Chiller with Parallel Flow

Energy Analysis	Exergy Analysis

Q_e = 16 kW	**Exergy Destruction**		**Exergy Loss**
Q_a = -24.18 kW	ED_a = 1.171 kW	ED_c = 0.1202 kW	EL_a = 0.3203 kW
Q_c = -7.47 kW	ED_e =0.2959 kW	ED_{hg} = 0.6312 kW	EL_c = 0.358 kW
Q_{hg} = 15.65 kW	ED_{lg} = 0.2663 kW	$ED_{valve,h}$ = 0.05195 kW	Total EL = 0.6783 kW
W_p = 0.003698	$ED_{vavle,m}$ = 0.0849 kW	$ED_{valve,s,h}$ = 0.0015 kW	**Total Irreversibility =Total ED + Total EL = 3.9743 kW**
	$ED_{valve,s,m}$ = 0.0014 kW	ED_{HTHX} = 0.4791 kW	
	ED_{LTHX} = 0.1922 kW	Total ED = 3.296 kW	**(also equals Exi-Exo)**
Energy Balance	**Energy Accounting**		
Energy Input = $Q_{hg} + Q_e + W_p$ = 31.65 kW	Exergy Input $Ex_i = Q_{hg}(1-T_0/(T[13]+5))$= 4.883 kW		
Energy Output = $Q_a + Q_c$ = 31.65 kW	Exergy Output $Ex_o = Q_e \|1-T_0/(T[10]+5)\|$ = 0.9086 kW		
COP = Q_e/Q_g = 1.022	**Exergetic Efficiency = Ex_o/Ex_i = 18.61 %**		
COP_{rev} = COP/Exergetic Efficiency = 5.49			

4.4 Double Effect Absorption Chiller with Series flow (Solution to HTRG first)

As in Section 4.3, the conservation equations and exergy rate balance equations were applied to the components in the double effect absorption chiller with series flow, where the solution flows to the HTRG first. The calculated results are shown in Table 4, and the resultant energy and exergy outputs and calculations are shown in Table 5. The reference points correspond to those in Figure 2.

Table 4: State Points in Double Effect Absorption Chiller with Series Flow (Solution to HTRG first, bold numbers are assumptions)

	P[kPa]	T[C]	X[%LiBr]	M[kg/sec]	H[kJ/kg]	S[kJ/kgK]
1	0.8136	**34**	55.35	0.1231	83.57	0.2044
2	130.1	34	55.35	0.1231	83.65	0.2044
3	130.1	58.91	55.35	0.1231	134.1	0.363
4	9.59	**88**	58.64	0.1162	204.5	0.5071
5	9.59	61	58.64	0.1162	151	0.3534
6	0.8136	61	58.64	0.1162	151	0.3535
7	9.59	74.1		0.004205	2638	8.33
8	9.59	45		0.006898	188.4	0.6385
9	0.8136	4		0.006898	188.4	0.6802
10	0.8136	**4**		0.006898	2508	9.049
11	130.1	106.4	55.35	0.1231	233.7	0.6418
12	130.1	**155**	56.59	0.1204	339.1	0.8819
13	130.1	107	56.59	0.1204	237.3	0.6312
14	9.59	107	56.59	0.1204	237.3	0.6313
15	130.1	**155**		0.002693	2784	7.511
16	130.1	107.2		0.002693	449.3	1.387
17	9.59	45		0.002693	449.3	1.555

Table 5: Energy/ Exergy Calculations for Double Effect Absorption Chiller with Series Flow (Solution to HTRG first)

Energy Analysis	**Exergy Analysis**	
Q_e = 16 kW	**Exergy Destruction**	**Exergy Loss**

Q_a = -24.56 kW	ED_a = 0.8925 kW	ED_c = 0.1023 kW	EL_a = 0.3254 kW
Q_c = -11 kW	ED_e =0.2958 kW	ED_{hg} = 0.6676 kW	EL_c = 0.5273 kW
Q_{hg} = 19.56 kW	ED_{lg} = 0.4329 kW	$ED_{valve,h}$ = 0.1351 kW	Total EL = 0.8527 kW
W_p = 0.009822	$ED_{vavle,m}$ = 0.08575 kW	$ED_{valve,s,h}$ = 0.0036 kW	**Total Irreversibility =Total ED + Total EL = 5.1997 kW**
	$ED_{valve,s,m}$ = 0.0035 kW	ED_{HTHX} = 1.234 kW	
	ED_{LTHX} = 0.4941 kW	Total ED = 4.347 kW	**(also equals Exi-Exo)**
Energy Balance	**Energy Accounting**		
Energy Input = $Q_{hg} + Q_e + W_p$ = 35.57 kW	Exergy Input $Ex_i = Q_{hg}(1-T_0/(T[12]+5))$= 6.108 kW		
Energy Output = $Q_a + Q_c$ = 35.56 kW	Exergy Output $Ex_o = Qe\ \|1-T_0/(T[10]+5)\|$ = 0.9086 kW		
COP = Q_e/Q_g = 0.818	**Exergetic Efficiency = Ex_o/Ex_i = 14.86 %**		
COP_{rev} = COP/Exergetic Efficiency = 5.5			

4.5 Double Effect Absorption Chiller with Series flow (Solution to LTRG first)

Finally, the same procedures were undertaken for the double effect absorption chiller with series flow, where the solution flows to the LTRG first. The calculated results for each state point are shown in Table 6, and the energy and exergy values and calculations are shown in Table 7. Again, the reference points in the tables correspond to those shown in Figure 3.

Table 6: State Points in Double Effect Absorption Chiller with Series Flow (Solution to LTRG first, bold numbers are assumptions)

	P[kPa]	T[C]	X[%LiBr]	M[kg/sec]	H[kJ/kg]	S[kJ/kgK]
1	0.8136	**34**	55.35	0.05163	83.57	0.2044
2	9.59	34	55.35	0.05163	83.57	0.2044
3	9.59	68.34	55.35	0.05163	153.6	0.4207
4	74.21	121.5	63.89	0.04473	292.7	0.6621
5	74.21	77.75	63.89	0.04473	211.9	0.4178
6	0.8136	77.75	63.89	0.04473	211.9	0.4179
7	9.59	68.5		0.002892	2627	8.299
8	9.59	45		0.006898	188.4	0.6385
9	0.8136	4		0.006898	188.4	0.6802
10	0.8136	**4**		0.006898	2508	9.049
11	9.59	**88**	58.64	0.04873	204.5	0.5071
12	74.21	88	58.64	0.04873	204.5	0.5071
13	74.21	116.8	58.64	0.04873	262.9	0.662
14	74.21	**155**	0.6389	0.04473	356.3	0.7892
15	74.21	**155**		0.004006	2788	7.777
16	74.21	91.5		0.004006	383.2	1.21
17	9.59	45		0.004006	383.2	1.323

Table 7: Energy/ Exergy Calculations for Double Effect Absorption Chiller with Series Flow (Solution to LTRG first)

Energy Analysis	**Exergy Analysis**		
Q_e = 16 kW	**Exergy Destruction**		**Exergy Loss**
Q_a = -22.46 kW	ED_a = 1.137 kW	ED_c = 0.03719 kW	EL_a =0.2975 kW
Q_c = -7.832 kW	ED_e =0.2958 kW	ED_{hg} = 0.3528 kW	EL_c = 0.3753 kW

<table>
<tr><td>Q_{hg} = 14.29 kW</td><td>ED_{lg}
= 0.2043 kW</td><td>$ED_{valve,h}$
= 0.1356 kW</td><td>Total EL
= 0.6728 kW</td></tr>
<tr><td>$W_p = Wp_{lm}+Wp_{mh}$
= 0.0047 kW</td><td>$ED_{vavle,m}$
= 0.08575 kW</td><td>$ED_{valve,s}$
= 0.00133 kW</td><td rowspan="3">Total Irreversibility
=Total ED + Total EL
= 3.55 kW

(also equals Ex_i-Ex_o)</td></tr>
<tr><td></td><td>ED_{HTHX}
= 0.556 kW</td><td>ED_{LTHX}
=0.07178 kW</td></tr>
<tr><td></td><td colspan="2">Total ED
= 2.878 kW</td></tr>
<tr><td>Energy Balance</td><td colspan="3">Energy Accounting</td></tr>
<tr><td>Energy Input
= $Q_{hg} + Q_e + W_p$ = 30.3 kW</td><td colspan="3">Exergy Input
$Ex_i = Q_{hg}(1-T_0/(T[14]+5))$= 4.456 kW</td></tr>
<tr><td>Energy Output
= $Q_a + Q_c$ = 30.29 kW</td><td colspan="3">Exergy Output
$Ex_o = Q_e\ |1-T_0/(T[14]+5)|$ = 0.9086 kW</td></tr>
<tr><td>COP = Q_e/Q_g = 1.119</td><td colspan="3">Exergetic Efficiency = Ex_o/Ex_i = 20.39 %</td></tr>
<tr><td colspan="4">COP_{rev} = COP/Exergetic Efficiency = 5.49</td></tr>
</table>

5 DISCUSSION

5.1 Gap between the Real COP and Theoretical Reversible COP

In Section 4, one can observe that there is a clear gap between the real COP (between 0.818 and 1.119) and the theoretical COP of 5.5 under the same set of environmental temperatures. This gap results from the entropy generation (exergy destruction in the system and loss to the environment). The lower the entropy generation in the whole process, the higher the exeregetic efficiency and the higher the real COP.

5.2 Exergy Destruction at the Component Level

In order to increase the real COP and exergetic efficiency, one must first diagnose the exergy destruction in each component in the absorption chiller systems. From Sections 4.3-4.5, it can be seen that the exergy destruction values vary among three different cycle configurations. However, when this is examined from a proportional viewpoint, as for the stacked exergy destruction shown in Figure 5, it can be observed that the absorber, high temperature regenerator and high temperature heat exchanger together share around 70% of the total exergy destruction in the absorption cycles. At the same time, the low temperature regenerator and low temperature heat exchanger share another 20% of the total exergy destruction. Research efforts into improving the COP should be focused on the highest exergy destruction components, namely the absorber, high temperature regenerator, and high temperature heat exchanger, to improve the system performance via entropy generation minimization.

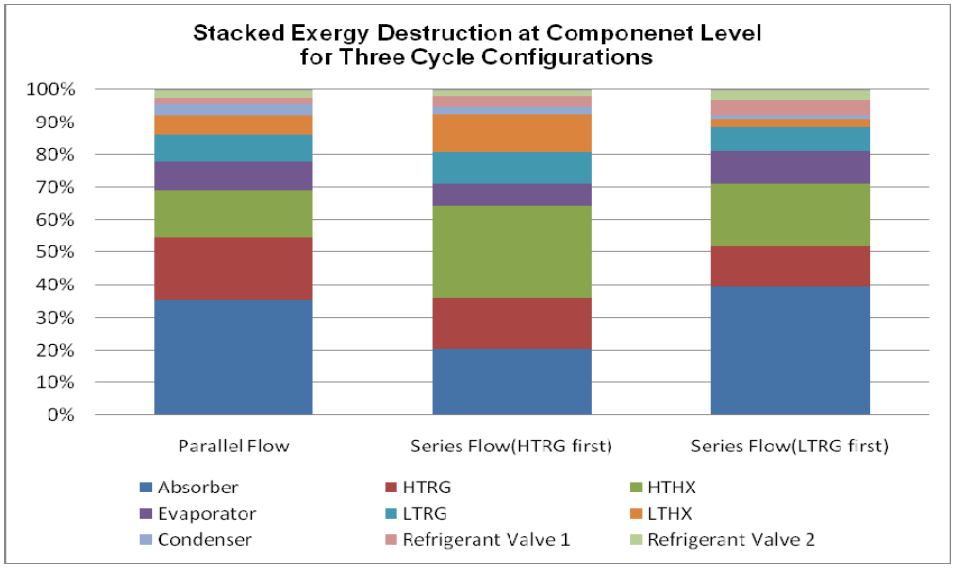

Figure 5: Stacked Exergy Destruction at Component Level for Three Cycle Configurations

5.3 Operational Issues and Configuration Selection

Given the same room, environmental, and regenerator temperatures, and under the same cooling capacity, the results presented in Sections 4.3-4.5 show that the series flow configuration where the solution flows to the low temperature regenerator first has the highest COP (COP=1.119), compared to the parallel flow configuration (COP=1.022) and the series flow configuration where the solution flows to the high temperature regenerator first (COP=0.8181). As expected, this is also the ordering of the configurations' exergetic efficiency values, from highest to lowest.

However, these values are not the only factor in choosing an "optimum" system. In real operation, for a cycle using a lithium bromide solution, the cycle parameters (mass fractions, temperatures, etc.) must always be set so as to avoid crystallization. The aqueous lithium bromide phase diagram is presented in Figure 6. According to the figure, for the series flow to the low temperature heat exchanger configuration, point 5 (77.89 C and 63.89% mass fraction) in the medium pressure level at the outlet of the low temperature heat exchanger is vulnerable to form crystallization in the heat exchanger and jam the piping.

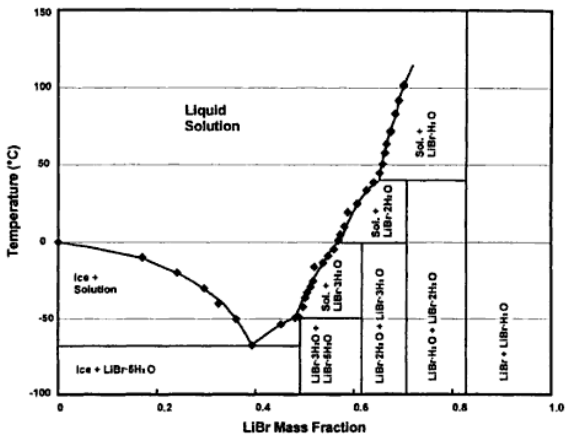

Figure 6: Aqueous Lithium Bromide Phase Diagram (Herold et al. 1996)

Fortunately, this problem does not exist for the conditions exhibited in the parallel flow configuration or the series flow with the solution entering the high temperature heat exchanger configuration. Therefore, in real applications, the parallel flow configuration is the most desirable to implement. This is not only because it has a competitively high COP (COP = 1.022), but also because the parallel flow can realize better matching conditions between the mass fraction and temperature.

6 CONCLUSION

In this paper, energy and exergy analyses for three double effect absorption chiller configurations are presented. Given the same cooling capacities and same environmental temperatures, the parallel absorption chiller exhibits the best behaviour among the three in terms of both the system performance and avoidance of crystallization. The exergy analysis shows that the exergy destructions for the generator, absorber, and heat exchangers are significantly larger than those in evaporator, condenser, and expansion valves. In order to achieve a higher level of performance, research and development must therefore focus on exergy destruction minimization (entropy generation minimization) of the generator, absorber and heat exchangers.

7 NOMENCLATURE

e = specific flow exergy	[kJ/kg]	ED = exergy destruction	[kW]
EL= exergy loss to environment	[kW]	Ex = exergy	[kW]
h = enthalpy	[kJ/kg]	$\dot{m}$ = mass flow rate	[kg/s]
P = Pressure	[kPa]	Q = heat absorbed or rejected	[kW]
S = entropy	[kJ/kgK]	T_0 = reference temperature	[K]
T = temperature	[K]	W = Work done to the system	[kW]
X = lithium bromide mass fraction	[%]		

Subscript

a = absorber	c = condenser
e = evaporator	hg = high temperature regenerator
lg = low temperature regenerator	i = inlet
o = outlet	rev = reversible process

HTHX =high temperature heat exchanger

LTHX = low temperature heat exchanger

valve,h = refrigerant valve from high to medium pressure

valve,m = refrigerant valve from medium to low pressure

valve,s,h = solution valve from high to medium pressure

valve,s,m = solution valve from medium to low pressure

8 REFERENCE

Herold K.E., Radermacher R., Klein S.A. 1996. Absorption chillers and heat pumps, CRC Press.

Lee S.F., Sherif S.A.,1999. “Second law analysis of multi effect lithium bromide/water absorption chillers,” *ASHRAE Transactions*; Ch-99-23-3: pp,1256-1266.

Arun MB, Maiya MP, Murthy SS, 2001. “Performance comparison of double effect parallel flow and series flow water lithium bromide absorption systems.” *Applied Thermal Engineering* Vol 21, pp,1273–1279.

Klein, S. A. and Alvarado, F. L. Engineering Equation Solver, 1992-2010 (F-Chart Software, Maddleton, Wisconsin).

BCT16 Manual, Broad Air Conditioning, 2005.

Patek, J. and Klomfar, J. 2006. “A computationally effective formulation of the thermodynamic properties of LiBr–H2O solutions from 273 to 500 K over full composition range”, International Journal of Refrigeration, Vol. 29, pp. 566-578.

Arora A., Kaushik S.C. 2009. “Theoretical analysis of LiBr/H2O absorption refrigeration systems,” *International Journal of Energy Research*, Vol. 33, pp 1321-1340.